

Yigit U., et al., Antifungal activity and optimization procedure of silver nanoparticles green synthesized with *Prunus laurocerasus* L. (cherry laurel) leaf extract. International Journal of Life Sciences and Biotechnology, 2023. 6(1): p. 1-20. DOI: 10.38001/ijlsb.1168628

Antifungal activity and optimization procedure of silver nanoparticles green synthesized with *Prunus laurocerasus* L. (cherry laurel) leaf extract

Ugür Yigit¹ , Yaren Gurel¹ , Hasan İlhan² , Muharrem Türkkan^{1,*} 

ABSTRACT

In this study, green synthesis conditions of silver nanoparticles (AgNPs) synthesized with *Prunus laurocerasus* (cherry laurel) leaf extract as reducing and coating agent were optimized using Box-Behnken design (BBD). Three important synthesis factors such as the concentration (M) of silver nitrate (AgNO₃), pH of cherry laurel leaf extract, and reaction temperature (°C) were used as independent variables of the model, and the absorbance intensity originating from AgNPs was employed as a dependent variable. Statistical analyzes showed that the optimized conditions for the predicted absorbance at 405 nm (2.35 A.U) were determined at a concentration of 0.01 M AgNO₃, a pH of 9.0, and a temperature of 50°C. The validity of the developed model was verified, and the average absorbance from six experimental runs was recorded as 2.26 (A.U) with an error of 14.86%. The synthesized AgNPs were characterized using Ultraviolet–Visible (UV–Vis) Spectroscopy, Fourier Transform Infrared (FT–IR) Spectroscopy, and Scanning Electron Microscopy–Energy Dispersive X-ray Spectroscopy (SEM–EDS). In addition, *in vitro* trials revealed that the synthesized AgNPs exhibited antifungal activity against all five fungal kiwifruit pathogens tested. The EC₅₀ values of synthesized AgNPs were 10.88, 9.30, 7.15, 25.16, and 53.77 µg/ml for *Phytophthora vexans*, *Globisporangium sylvaticum*, *G. intermedium*, *Phytophthora citrophthora*, and *Rhizoctonia solani*, respectively. With the exception of the MIC values of two *Globisporangium* species (120 µg/ml), both MIC and MFC values of the remaining three species were found to be above 150 µg/ml. The results of this study indicate that AgNPs synthesized with cherry laurel leaf extract should be further investigated for use in the control of fungal root and stem rot diseases in kiwifruit.

ARTICLE HISTORY

Received

09 September 2022

Accepted

04 December 2022

KEYWORDS

Prunus laurocerasus, silver nanoparticle, Box-Behnken design, antifungal activity

Introduction

Today, silver (Ag) nanoparticles (NPs) are of great interest due to their optical, catalytic, mechanical, electrical, and biosensing properties [1, 2, 3]. AgNPs also have strong antimicrobial activity and are widely used in the pharmaceutical industry as an ingredient in the preparation of human health drugs [4]. In many studies, it has been shown that AgNPs can be synthesized by chemical and physical methods, but it has become

¹ Ordu University, Faculty of Agriculture, Department of Plant Protection, 52200 Ordu, Turkey

² Ordu University, Faculty of Science, Department of Chemistry, 52200 Ordu, Turkey

*Corresponding Author: Muharrem Türkkan, e-mail: muhammetturkkan@gmail.com; muhammetturkkan@odu.edu.tr

necessary to find an alternative method due to the use of large amounts of toxic chemicals in the synthesis process [5, 6, 7, 8, 9, 10, 11]. On the other hand, the biological approach based on living organisms (bacteria, fungi, lichens, plants, etc.) offers a reliable, simple, rapid, non-toxic, and environmentally friendly solution [12, 13, 14, 15]. Among these bio-resources, plants are more popular as they are readily accessible, non-toxic, and easily processed. Plants also have many biologically active compounds such as polyphenols, organic acids, and proteins that serve not only as reducing agents but also as capping agents making synthesis an easy process [16, 17]. The green synthesis of nano-sized silver nanoparticles using alfalfa sprouts (variety Mesa) was first reported by Gardea-Torresdey [18]. Recently, extracts of various plant parts such as leaves, flowers, fruits, rhizomes, seeds, etc. have been successfully used in the synthesis of AgNPs. *Azadirachta indica* (leaf extract) [1], *Aloe vera* (leaf extract) [1], *Camellia sinensis* (plant extract) [21], *Cinnamon zeylanicum* (bark extract) [22], *Jatropha curcas* (seed extract) [23], *Musa paradisiaca* (peel extract) [24], *Acalypha indica* (leaf extract) [25], *Macrotyloma uniflorum* (seed extract) [26], *Prosopis juliflora* (leaf extract) [27], *Pimenta dioica* (leaf extract) [28], *Alstonia scholaris* (bark extract) [29], *Eucalyptus oleosa* (plant extract) [30], *Artemisia absinthium* (leaf extract) [31], *Atrocarpus altilis* (leaf extract) [32], *Camellia japonica* (leaf extract) [33], *Rubus glaucus* (fruit extract) [34], *Nigella arvensis* (leaf extract) [35], *Prosopis juliflora* (bark extract) [36], *Pueraria tuberosa* (tuber extract) [37], *Berberis vulgaris* (leaf and root extracts) [38], *Erodium cicutarium* (plant extract) [39], *Teucrium polium* (stem and flower extracts) [40], *Zingiber officinale* (rhizome extract) [41], *Clitoria ternatea* (flower extract) [42], *Diospyros malabarica* (fruit extract) [43], *Malva parviflora* (leaf extract) [44], and *Psidium guajava* (leaf extract) [45] are examples of plants used in AgNPs synthesis. Of these, the AgNPs synthesized with extracts of *A. absinthium* and *M. parviflora* have been shown to be a potent inhibitor against *Alternaria alternata*, *Helminthosporium rostratum*, *Fusarium solani*, *F. oxysporum*, *Phytophthora capsici*, and *P. parasitica* [31, 44]. In addition, several others have been reported to exhibit antibacterial activity [22, 25, 38].

Prunus laurocerasus L. (cherry laurel), which belongs to the Rosaceae family, is an evergreen shrub or small tree native to Europe, the Caucasus, Iran and Türkiye [46]. Cherry laurel is cultivated in the Black Sea region of Türkiye for its fruits and is known as Karayemiş or Taflan. In Turkish traditional medicine, cherry laurel leaves are used in

the treatment of asthma, coughs, and dyspepsia [47, 46]. Şahan also determined that aqueous and ethanolic extracts of cherry laurel leaves have antifungal activity against various bread molds (*Aspergillus*, *Mucor*, *Penicillium*, and *Rhizopus*) [48]. Previous studies have shown that cherry laurel is a rich source of various biochemicals such as protein, sugar, ascorbic acid, minerals, and antioxidants [46, 48]. Furthermore, Karabegovic et al. determined that both leaf and fruit extracts contain high amounts of phenolic and flavonoid compounds [49]. Thus, these compounds may serve to produce AgNPs by mediating the reduction of silver ions.

Response surface methodology (RSM), a statistical and graphical technique, is a widely used methodology for designing models and analyzing various manufacturing problems [50]. RSM helps to identify factors, examine interactions and optimal conditions, compute the optimum level of variables, and ensure maximum production in a constant number of experiments.

In this study, silver nanoparticles synthesized using cherry laurel leaf extract were optimized using Box-Behnken design (BBD). AgNPs synthesized under optimized conditions were characterized by Ultraviolet–Visible (UV–Vis) Spectroscopy, Fourier Transform Infrared (FT–IR) Spectroscopy, and Scanning Electron Microscopy–Energy Dispersive X-ray Spectroscopy (SEM–EDS). In addition, their antifungal activities on some important fungal disease agents that cause root and stem rot in kiwifruits were evaluated under *in vitro* conditions in the laboratory.

Material and Methods

Plant material, chemicals, and fungal cultures

The leaves of *Prunus laurocerasus* (cherry laurel) were collected from Gülyalı district of Ordu, Türkiye (40°57'58.8"N 38°00'00.4"E).

Silver nitrate (AgNO₃), sodium hydroxide (NaOH) and hydrochloric acid (HCl) from Merck (Darmstadt, Germany), and potato dextrose agar (PDA) medium were purchased from BD Difco (Sparks, MD, USA).

Phytophthora vexans, *Globisporangium sylvaticum*, *G. intermedium*, *Phytophthora citrophthora*, and *Rhizoctonia solani* AG 4 HG-I isolates causing root and stem rot in kiwifruit were obtained from fungal culture collection of the Faculty of Agriculture, Department of Plant Protection, Mycology Laboratory (Ordu University).

Preparation of plant extract

Cherry laurel leaves were surface cleaned with running tap water to remove the debris, then washed with distilled water and dried with a paper towel. Afterward, they were dried in an oven at 60°C for 4 days and ground into a fine powder using a blender. Twenty grams of the leaf powder were mixed with 100 ml of distilled water in a 500 ml flask and stirred continuously for 30 min at 80°C using a heater stirrer. After cooling, the extracts were centrifuged and filtered through Whatman No. 1 filter paper and then kept in a refrigerator at 4°C.

Green synthesis of AgNPs

In this experiment, solutions of AgNO₃ in distilled water at 0.001, 0.0055, and 0.01 M concentrations were prepared and used as the metal source (Ag) for AgNPs biosynthesis. To synthesize AgNPs, 10 ml of cherry laurel leaf extracts at different pHs (5, 7, and 9) was added to 90 ml of the above aqueous solutions and vigorously stirred at various temperatures (25, 50, and 75°C) for 30 min. The reduction of Ag⁺ ions to Ag⁰ ions was confirmed by the color change from colorless to dark brown. The precipitates of each sample were obtained by centrifuging at 10000 rpm for 15 min. The collected NPs were washed three times with double distilled water and the washed samples were suspended in 5 ml of distilled water.

Statistical optimization of AgNPs synthesis

Box-Behnken design (BBD) from RSM was used to evaluate the effect of independent variables (silver nitrate concentration, pH of plant leaf extract, and reaction temperature) on the synthesis of AgNPs and also to find an optimum condition. Each variable was coded at three levels of +1 (high), 0 (middle) and -1 (low) (**Table 1**). A Box-Behnken was designed, consisting of a total of 17 runs with five repetitions at the central point (**Table 2**). The following quadratic polynomial equation was used to compute the relationship between the three independent variables and the response.

$$Y = \beta_0 + \beta_1 A + \beta_2 B + \beta_3 C + \beta_{11} A^2 + \beta_{22} B^2 + \beta_{33} C^2 + \beta_{12} AB + \beta_{13} AC + \beta_{23} BC$$

where Y is the predicted response (predicted absorbance of AgNPs), A, B, and C are the independent variables, β_0 is the regression coefficient at center point, β_1 , β_2 , and β_3 are the linear coefficient; β_{11} , β_{22} , and β_{33} are the quadratic coefficients, and β_{12} , β_{13} , and β_{23} are the second order interaction coefficients.

All analyzes were performed with version 13 of the Design Expert program (Stat-Ease, Inc., USA). The program was used for regression analysis of the data obtained and to estimate the regression equation coefficient. The fitted model was then plotted in the form of perturbation, 3D response surface, and 2D contour plots to illustrate the relationship between responses. Finally, experimental sets were made using the suggested optimum combination to validate the developed model.

Table 1 Level of variables chosen for Box-Behnken design

Coded factor	Variables	Units	Minimum	Maximum	Coded Low	Coded High	Mean	Std. Dev.
A	AgNO ₃ concentration	M	0.001	0.01	-1 ↔ 0.001	+1 ↔ 0.01	0.0055	0.0032
B	pH of cherry laurel leaf extract	-	5.00	9.00	-1 ↔ 5.00	+1 ↔ 9.00	7.00	1.41
C	Reaction temperature	°C	25.00	75.00	-1 ↔ 25.00	+1 ↔ 75.00	50.00	17.68

Table 2 Experimental design using Box-Behnken showing coded and actual values along with the experimental and predicted responses

Run order	AgNO ₃ concentration (M)	pH of cherry laurel leaf extract	Reaction temperature (°C)	Absorbance (405 nm)	
				Actual	Predicted
1	-1	0	-1	0.5857	0.7601
2	1	0	1	1.7246	1.5500
3	0	0	0	1.5988	1.6600
4	0	1	1	1.8395	1.9600
5	0	0	0	1.7943	1.6600
6	1	0	-1	1.7112	1.7100
7	1	-1	0	0.3532	0.4772
8	0	-1	-1	1.1539	1.0300
9	0	0	0	1.5968	1.6600
10	-1	1	0	0.7398	0.6158
11	1	1	0	2.2945	2.3500
12	-1	0	1	0.6021	0.6046
13	0	1	-1	2.1188	2.0700
14	-1	-1	0	0.3674	0.3145
15	0	0	0	1.5703	1.6600
16	0	-1	1	0.7753	0.8257
17	0	0	0	1.7173	1.6600

Characterization of AgNPs

UV–Vis analysis of the synthesized AgNPs was performed with a UV–Vis Spectrometer (Lambda 35, Perkin Elmer, Inc., MA, USA). A 200 µl solution containing AgNPs was

diluted with 2 ml of distilled water. The spectra of AgNPs were obtained in the wavelength range of 200-700 nm at 1 nm resolution using a quartz cuvette. Baseline correction was done using distilled water as the blank.

Infrared spectra of the AgNPs were recorded on Fourier Transform Infrared (FT-IR) Spectroscopy (Spectrum 65, Perkin Elmer, Inc., MA, USA). One mg of the synthesized NPs was mixed with 200 mg KBr, then pressed into a pellet. FT-IR spectra from the nanoparticles were collected at the wave number range of 4000-400 cm^{-1} in the transmittance mode.

Chemical composition and morphology analysis of the AgNPs were carried out using a Hitachi Scanning Electron Microscope (SEM) (SU-1510, Hitachi High-Technologies Corp., Tokyo, Japan) coupled with Energy Dispersive X-ray Spectroscopy (EDS).

Antifungal effect of the synthesized AgNPs on fungi

Antifungal activities of the synthesized AgNPs against the fungi were tested according to Türkkan with a minor modification [51].

Different concentrations of AgNPs (15, 30, 60, 90, 120, and 150 $\mu\text{g/ml}$) were added to autoclaved and then cooled PDA medium at 55°C. A 15 ml aliquot of modified PDA medium was aseptically dispensed into a Petri plate (8-cm-dia.), with an unmodified PDA plate used as a control. A 5 mm diameter mycelial disc from 7-day-old fungal cultures was placed in the center of each plate and incubated at 25°C in the dark after sealing the plates with Parafilm. When control fungal colonies covered plates (2-7 days), all colony diameters were measured at two perpendicular points. The growth values were converted into percent inhibition of the mycelial growth inhibition (MGI) in relative to controls using the formula $\text{MGI} (\%) = [(dc - dt)/dc] \times 100$, where dc represents the fungal growth diameter of the control and dt represents the fungal growth diameter of the modified plates. The experiment was performed twice with 3 replications for each fungus.

Probit analysis (IBM SPSS Statistics, Version 22; IBM Company, Chicago, USA) was used to compute the concentrations of the AgNPs that caused a 50% reduction (EC_{50}) in mycelial growth of the fungi. The minimum inhibitory concentration (MIC) value, which totally inhibited mycelial growth, was also found by parallel experiments.

Toxicity (fungistatic/fungicidal) of the AgNPs was evaluated according to Thompson and Tripathi et al. [52, 53]. PDA discs taken from modified plates that exhibited no fungal growth were re-inoculated with unmodified PDA plates and then monitored for 9 days at

25°C revivals of growth. At the end of this period, the minimum AgNPs concentration required to completely and irreversibly inhibit fungal growth was recorded as the minimum fungicidal concentration (MFC) value.

Results and Discussion

Optimization of process parameters by response surface methodology (RSM)

In this study, the Box-Behnken design was used to determine the optimum experimental condition for the synthesis of AgNPs. Considering the peak intensity, three independent synthesis factors including the concentration of AgNO₃ solution, pH of the plant leaf extract, and reaction temperature were investigated to obtain the optimal surface plasmon resonance (SPR) band of the synthesized AgNPs.

In preliminary studies, pH was shown to be one of the most effective variables in the synthesis of AgNPs. Therefore, a series of syntheses were performed to determine the pH range in the research, with a one-at-a-time approach based on varying the pH (4-10) and constant amounts of other two factors (AgNO₃ = 0.001 M and temperature = 50°C). Silver nanoparticle synthesis occurred in the pH range of 5-10 but did not produce SPR as AgNP was suppressed at pH 4 (**Fig 1**). Furthermore, a fairly broad SPR peak (470 nm) was observed at pH 5.0; this may be related to the agglomeration of NPs at acidic pH, which results in an increase in the size of the NPs [54]. In contrast, at pH 9.0, a relatively narrow SPR peak was observed with λ_{max} at 405 nm which can be due to an increase in the small diameters of nanoparticles. Veerasamy et al. reported that high pH values facilitate the binding of more AgNPs with many functional groups available for silver bonding [55]. Vanaja et al. also stated that nanoparticle formation was ascended with increasing pH [54]. Therefore, the pH values (5, 7, and 9) of acidic, neutral, and alkaline solutions were used in the Box-Behnken design.

The Box-Behnken design for three factors was constituted with a total of 17 runs. The absorbance intensity of the SPR was used as the response of the Box-Behnken design and modeling resulting from the absorbance of 17 AgNP synthesized at 405 nm (**Table 2**).

In order to determine the optimal values of AgNP synthesis, the Design Expert program proposed a quadratic model to correlate the relationship between experimental factors and response. The developed model is expressed in terms of coded (1) and actual (2) factors as follows:

$$Y \text{ (Absorbance)} = 1.66 + 0.4736A + 0.5429B - 0.0785C - 0.5164A^2 - 0.2004B^2 + 0.0168C^2 +$$

$$0.3922AB - 0.0008AC + 0.0248BC \quad (1)$$

$$Y \quad (\text{Absorbance}) = -1.97563 + 81.00556A + 0.708307B - 0.009263C - 25500A^2 - 0.050100B^2 + 0.000027C^2 + 43.58056AB - 0.006667AC + 0.000496BC \quad (2)$$

Where Y is the obtained absorbance (405 nm) as an indication of the SPR intensity; A is silver nitrate concentration; B is pH value of plant leaf extract; and C is the reaction temperature.

The significance of this quadratic model was checked with an analysis of variance using the F-test (**Table 3**). The model F-value of 28.39 implies that the model is statistically significant. There is only a 0.01% chance that an F-value this large could occur due to noise while p-values are 0.0001. P-values less than 0.05 indicate that the developed quadratic model and model terms are significant. In this case, A, B, AB, A² and B² are significant model terms. The Lack of Fit F-value of 4.75 means that the Lack of Fit is negligible compared to pure error and is a good indicator for the model.

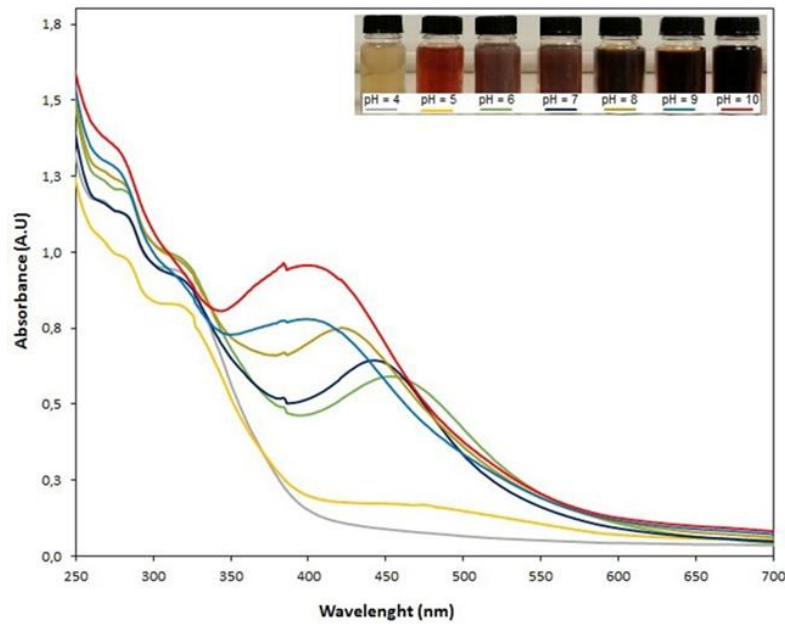


Fig 1 Visual observations and UV–Vis spectra of reaction mixtures with different pHs at fixed values of AgNO₃ concentration (0.001 M) and reaction temperature (50°C)

In our study, the regression coefficient ($R^2 = 0.9733$) means that 97.33% of both observed and predicted data can be explained by using this model (**Fig 2a, Table 4**). It is reported that a suitable statistical model should result in $R^2 \sim 1$ [56]. Adequate precision measures the signal-to-noise ratio, and a ratio greater than 4 is desirable. The ratio of 17.0674

indicated an adequate signal; hence, the model can be used to continue the design process. In the developed model, the residuals show a random distribution between the predicted and actual (observed) values, which shows that all the residual values lie along a straight line without large deviations, confirming the normality of the error distribution (**Fig 2b**). It is also shown in **Fig 2(c)** that not only is the residue randomly distributed on both sides of the zero line but is also within the acceptable range. Mondal and Purkait stated that the residuals between predicted and actual values should be in the range of $\pm 3\%$, demonstrating that the constructed model is sufficient [57]. The perturbation plot shows that AgNO₃ concentration (A) and pH of the plant leaf extract (B) have a large positive effect on increasing the amount of AgNP synthesis, but the effect of the reaction temperature (C) is quite limited (**Fig 2d**).

In the study, 3D response surface and 2D contour plots were used to show the interactions among variables and their mutual effects on the response (absorbance) (**Fig 3**). **Fig 3(a)** shows the relationship between AgNO₃ concentration (A) and pH of the plant leaf extract (B), which has a similar effect on the AgNPs synthesis. As can be seen, AgNPs synthesis was at its highest when both were increased. On the other hand, the increase in the reaction temperature (°C) limited the AgNPs synthesis to some extent.

Table 3 Analysis of variance (ANOVA) for quadratic model

Source	Sum of Squares	df	Mean Square	F-value	p-value	
Model	6.16	9	0.6847	28.39	0.0001	significant
A-AgNO ₃ concentration (M)	1.79	1	1.79	74.39	< 0.0001	
B-pH of cherry laurel leaf extract	2.36	1	2.36	97.75	< 0.0001	
C-Reaction temperature (°C)	0.0493	1	0.0493	2.04	0.1958	
AB	0.6154	1	0.6154	25.52	0.0015	
AC	2.25E-06	1	2.25E-06	0.0001	0.9926	
BC	0.0025	1	0.0025	0.1022	0.7585	
A ²	1.12	1	1.12	46.55	0.0002	
B ²	0.1691	1	0.1691	7.01	0.033	
C ²	0.0012	1	0.0012	0.0491	0.8309	
Residual	0.1688	7	0.0241			
Lack of Fit	0.1318	3	0.0439	4.75	0.0832	not significant
Pure Error	0.037	4	0.0093			
Cor Total	6.33	16				

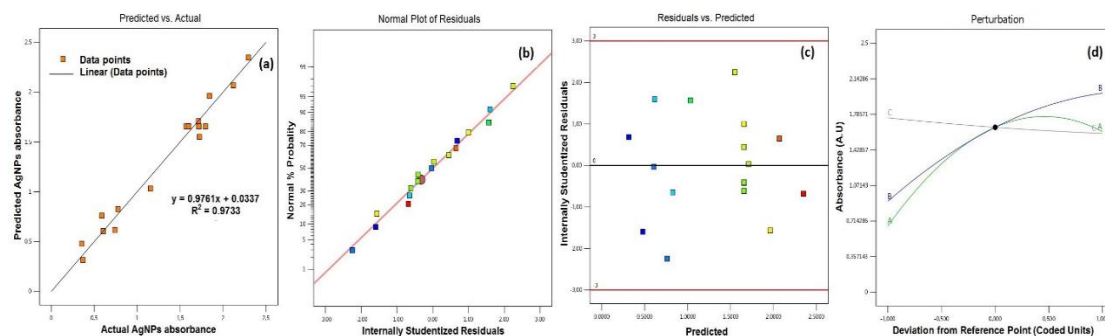


Fig 2 Diagnostic plots of AgNPs optimized using Box-Behnken design: (a) predicted versus actual, (b) normality of residuals, (c) residuals versus predicted, and (d) perturbation

Table 4. Fit and model summary statistics

Std. Dev.	0.1553	R ²	0.9733
Mean	1.33	Adjusted R ²	0.9391
C.V. %	11.71	Predicted R ²	0.6578
		Adeq Precision	17.0674
PRESS	2.17	-2 Log Likelihood	-30.16
BIC	-1.83	AICc	26.5

Depending on the other two variables, it is seen that they may lead to higher AgNP formation in the range of approximately 25-50°C (**Fig 3b; 3c**). Similarly, Sun et al. found that the increase in temperature did not have a significant effect on the production efficiencies of AgNPs [58]. Sanghi and Verma stated that silver ion reduction at higher pH was favorable and proceeded at a higher rate [59]. Furthermore, Nikaeen et al. reported that the interaction of pH and silver concentration has a greater effect on the synthesis of AgNPs than other factors such as reaction temperature and time [60].

In the present study, the optimum values of AgNO₃ concentration, cherry laurel leaf extract pH, and reaction temperature for the synthesis of AgNPs at 405 nm are 0.01 M, 9.0, and 50°C, respectively, and the absorbance value of the corresponding AgNPs is 2.35. We repeated the experimental synthesis of AgNPs using the parameters mentioned above and obtained an absorbance value of 2.26 with an error value of 14.86% (**Fig 4**), which is less than 20% (0.2) error value. Since the error value is lower than the standard value (0.2) of Design Expert software, it has been verified that it is sufficient for the optimization of the model parameters.

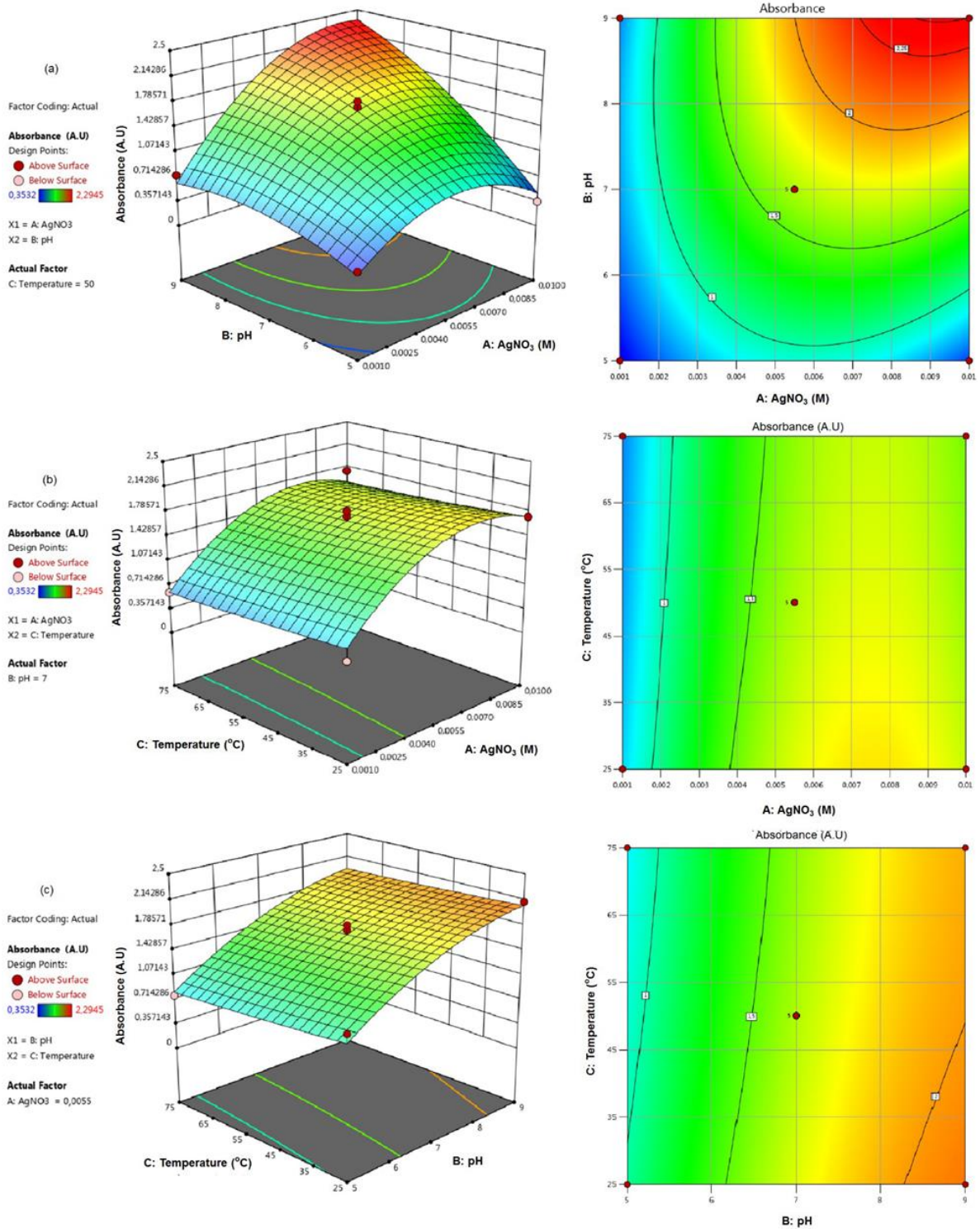


Fig 3 3D response surface and 2D contour plot for interaction effect of two-parameter on absorption response at fixed values of other parameters: (a) influence of AgNO₃ concentration and cherry laurel extract pH on absorbance, (b) influence of AgNO₃ concentration and reaction temperature on absorbance, and (c) influence of cherry laurel extract pH and reaction temperature on absorbance

Characterization of AgNPs

UV–Vis spectral analysis

The solutions containing different runs in the Box-Behnken design caused a wide color change, ranging from yellowish brown to dark brown, at the end of the reaction time (**Fig 5**). This color change indicates that the silver ions in the solution are reduced from Ag^{+1} to Ag^0 . It may be due to the excitation of the SPR [61], which is the typical feature of AgNPs. **Fig 5** shows the UV–Vis spectra of silver colloid as a function of the reactions of Ag ions with the plant leaf extract. The characteristic SPR bands of AgNPs in the study were observed between 405 and 472 nm, which was within the range previously reported for AgNPs [60, 62]. The different absorption spectra in the formation of AgNPs indicate the existence of different morphology and size variations [26].

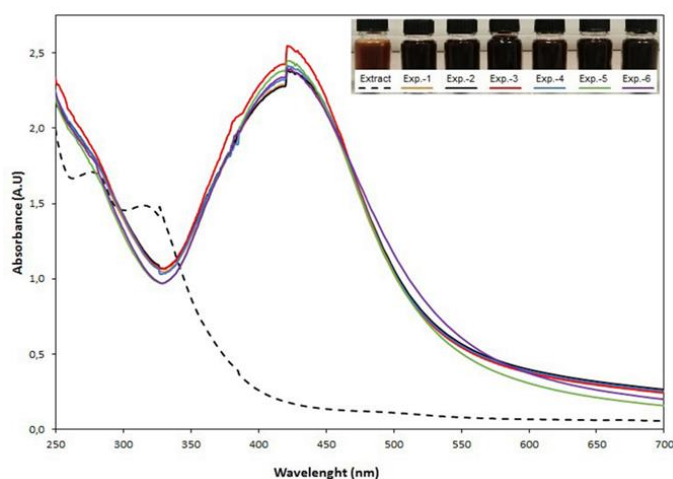


Fig 4 Visual observations and UV–Vis spectra of AgNPs synthesized by six experimental runs under optimum conditions

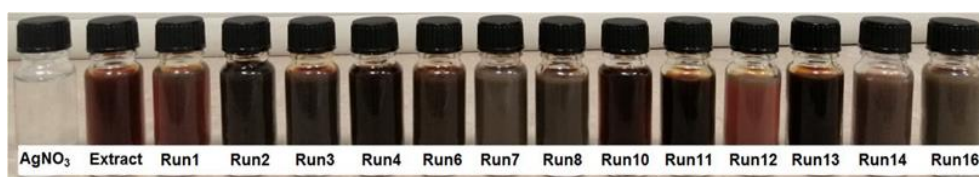


Fig 5 Changes in solution colors confirming the formation of AgNPs in different experimental runs

FT–IR studies

To get information about molecules and functional groups in newly synthesized AgNPs, an FT–IR spectrum was used. **Fig 6** illustrates the FT–IR spectrum of stabilized AgNPs. The spectra indicate nanoparticle absorption bands at about 3370, 2920, 1604, 1357, 1242, 1026, 832 and 601 cm^{-1} . Phenolic metabolites of cherry laurel leaf extract caused a

strong peak at 3370 cm^{-1} . The band at 2920 cm^{-1} was related to the stretching vibration of the alkane C–H bond. Perhaps the presence of the carbonyl group causes the C=O stretching. The C=C stretching vibration of aromatic rings was responsible for the peak at 1604 cm^{-1} . The C–N stretching of the aromatic amine group was shown by the peak at $1357, 1319\text{ cm}^{-1}$ in the spectrum. Furthermore, the peaks at 1242 and 1026 cm^{-1} were corresponded to C–N stretching, which occurred as a result of the presence of the amine groups. Another band at 832 cm^{-1} was typical of the aromatic ring. According to the results, cherry laurel leaf extract contained proteins, phenolic compounds, flavonoids, and aromatic groups, which were reported to be responsible for the reduction of Ag ions to nanoparticles [19, 63, 64, 65].

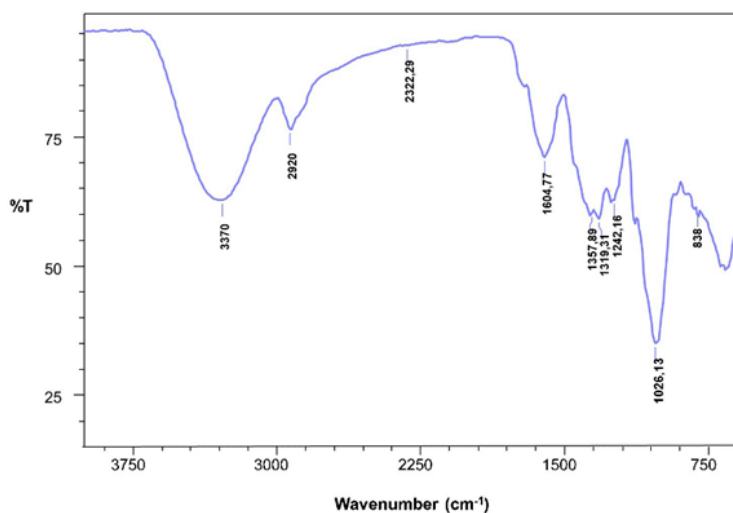


Fig 6 FT–IR spectra representing functional groups associated with cherry laurel leaf extract-mediated reduction and stabilization of silver ions

SEM–EDS analysis

The size, shape, and morphologies of the synthesized AgNPs were characterized by SEM. According to the SEM images of the silver nanoparticles (**Fig 7a**), the AgNPs had an almost spherical morphology, with an average particle size of 80.39 nm. It is possible to determine the composition and metal distribution of a sample using SEM and Energy Dispersive X-ray Spectroscopy (EDS). Because of the SPR of AgNPs, Magudapatty and groups demonstrated that optical absorption peaks of silver nanoparticles emerged at almost 3 keV [66]. AgNPs with a crystalline character were found to provide a peak in the 3 keV area in our EDS profiles (**Fig 7b**).

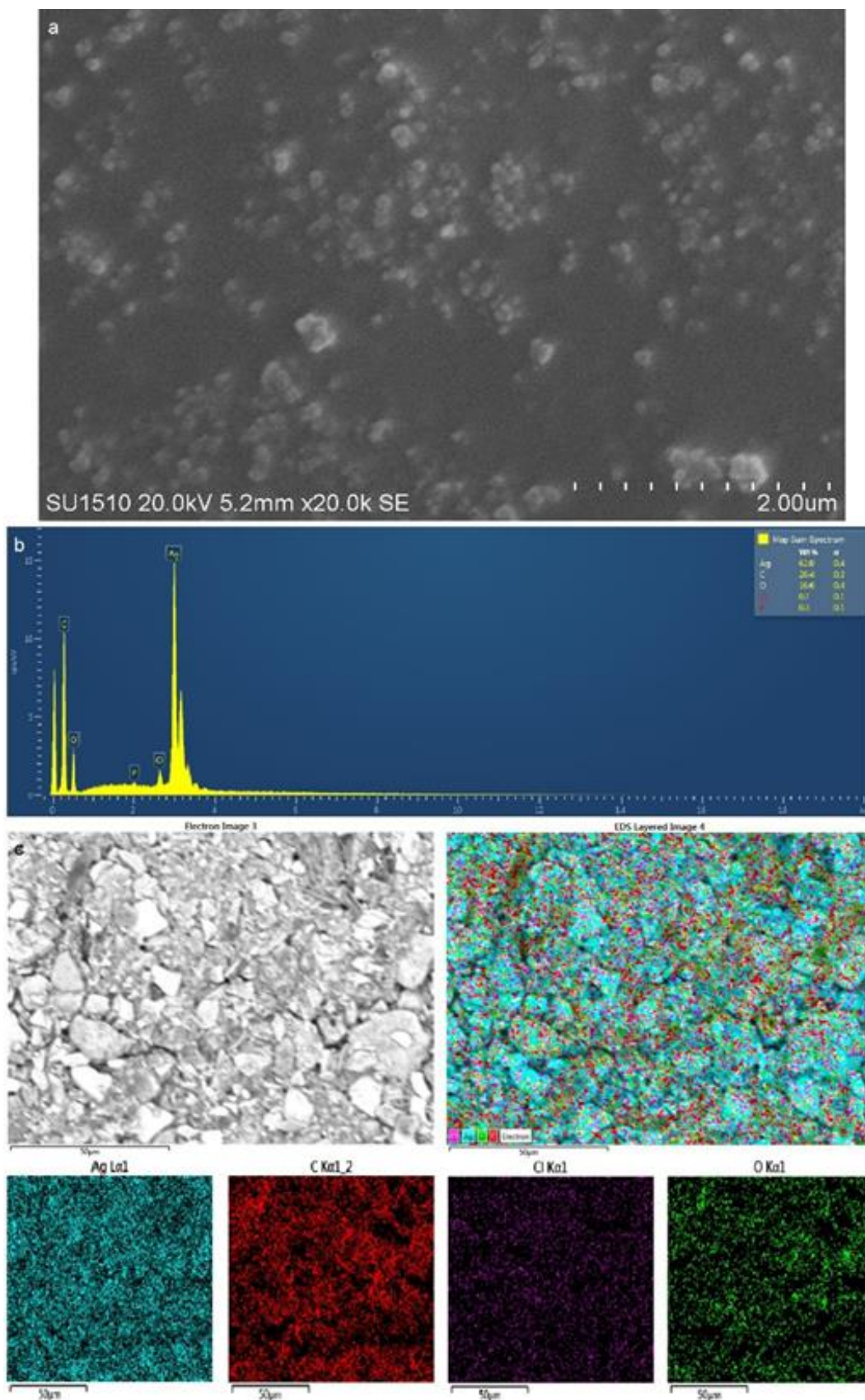


Fig 7 Element analysis and purity assessment of the synthesized AgNPs are based on (a) SEM images, (b) EDS spectrum, (c) SEM-EDS mapping approach

EDS spectra showed that oxygen (O), carbon (C), phosphorus (P), and chlorine (Cl) were found in the residual materials that surround NPs and the SEM grid that was used to prepare them. The synthesized AgNPs had a strong Ag atom signal compared to the signals from C, O, Cl, and P. **Fig 7(c)** displayed the EDS mapping of green synthesized AgNPs. The EDS mapping result for Ag, C, O, and Cl was shown in the image of respective blue, red, green, and purple colors. AgNPs were confirmed by the EDS elemental mapping analysis, which revealed a signal of Ag (blue). In addition, the SEM results showed that the particles are well dispersed and uniformly distributed.

Antifungal activity of the synthesized AgNPs

The results of the antifungal activity of AgNPs presented in **Table 5** show that the synthesized AgNPs reduced the mycelial growth of all five fungi tested. Among the fungi, *Globisporangium intermedium* was found to have the most sensitive against the synthesized AgNPs, followed by *G. sylvaticum* and *Phytophthium vexans*. The AgNPs at 120 µg/ml concentration completely inhibited *G. intermedium* and *G. sylvaticum*. However, this effect was observed to be fungistatic and re-developed when inoculums of both fungi were transferred to a fresh PDA medium. On the other hand, for the remaining three fungi (*P. vexans*, *Phytophthora citrophthora*, and *Rhizoctonia solani*), both MIC and MFC values of the synthesized AgNPs were greater than 150 µg/ml. In previous studies, it was found that AgNPs synthesized by biological method exhibited strong antifungal activity against various oomycetes (*Phytophthora capsici*, *P. cinnamomi*, *P. infestans*, *P. katsurae*, *P. palmivora*, *P. parasitica*, *P. tropicalis*) and fungi (*Alternaria alternata*, *Botrytis cinerea*, *Curvularia lunata*, *Helminthosporium rostratum*, *Fusarium solani*, *F. oxysporum*, *Macrophomina phaseolina*, *R. solani*, and *Sclerotinia sclerotiorum*) [31, 67, 44]. It is assumed that the antifungal activity of AgNPs is related to their very small structure, shape, and form and that AgNPs act by disrupting the normal functions of cell organelles after penetrating the microbial cell [68].

Table 5 EC₅₀, MIC and MFC values of the synthesized AgNPs inhibiting mycelial growth of kiwifruit fungal root and stem rot agents

Fungi	EC₅₀^a (µg/ml)	MIC^b (µg/ml)	MFC^c (µg/ml)
<i>Phytophthium vexans</i>	10.88	> 150.00	> 150.00
<i>Globisoprangium sylvaticum</i>	9.30	120.00	> 150.00
<i>G. intermedium</i>	7.15	120.00	> 150.00
<i>Phytophthora citrophthora</i>	25.16	> 150.00	> 150.00
<i>Rhizoctonia solani</i>	53.77	> 150.00	> 150.00

^aThe concentration that caused 50% reduction. ^bMinimum inhibitory concentration. ^cMinimum fungicidal concentration.

Conclusion

In this study, AgNPs were synthesized by a green method using cherry laurel (*Prunus laurocerasus*) leaf extract. Based on the RSM, the Box-Behnken design was used to optimize three important experimental parameters in the biosynthesis process of AgNPs, such as AgNO₃ concentration, pH of the plant leaf extract, and reaction temperature. The optimum conditions of the experimental parameters are computed as 0.01 M, pH 9.0, and 50°C through a three-factor Box-Behnken design with 17 runs and this reaction condition was experimentally verified. The synthesized AgNPs were characterized by UV–Vis, SEM–EDS, and FT–IR analyzes. In addition, the synthesized AgNPs exhibited antifungal activity against some kiwifruit fungal pathogens, such as *P. vexans*, *G. sylvaticum*, *G. intermedium*, *P. citrophthora*, and *R. solani*.

Abbreviations

AgNPs; silver nanoparticles; AgNO₃; silver nitrate; NaOH; sodium hydroxide; HCl; hydrochloric acid; PDA; potato dextrose agar; BBD; Box-Behnken design; RSM; response surface methodology; UV–Vis spectroscopy; ultraviolet–visible spectroscopy; FT–IR; fourier transform infrared spectroscopy; SEM; scanning electron microscopy; EDS; energy dispersive X-ray spectroscopy; SPR; surface plasmon resonance.

Acknowledgments

This report is a part of the Ph.D. thesis of Uğur Yiğit, Ph.D. candidate in Plant Protection Department, Ordu University. This study was supported by the Research Foundation of Ordu University, Project No: B-2209

Data Availability statement

The authors confirm that data supporting the findings of this study are available in the article and Supplementary material. All data are included in Uğur Yiğit doctoral (Ph.D.) thesis. Raw data supporting the findings of this study are available from the corresponding author upon reasonable request.

Compliance with ethical standards

Conflict of interest

The authors declare no conflict of interest.

Ethical standards

The study is proper with ethical standards

Authors' contributions

All authors contributed to the study's conception and design. Material preparation, data collection and analysis were performed by Uğur Yiğit, Yaren Gürel, and Muharrem Türkkkan. Muharrem Türkkkan wrote the original draft of the manuscript. Uğur Yiğit, and Hasan İlhan reviewed and edited the manuscript. All authors read and approved the final manuscript.

Consent to participate

Informed consent was obtained from all individual participants included in the study.

Consent to publish

The study does not include human and animal experiments.

References

1. Jain, P.K., et al., Noble metals on the nanoscale: optical and photothermal properties and some applications in imaging, sensing, biology, and medicine. *Accounts of Chemical Research*, 2008. 41: p. 1578–1586.

2. Tran, Q.H., and A.T. Le, Silver nanoparticles: synthesis, properties, toxicology, applications and perspectives. *Advances in Natural Sciences: Nanoscience and Nanotechnology*, 2018. 9: p. 049501.
3. Wei, L., et al., Silver nanoparticles: synthesis, properties, and therapeutic applications. *Drug Discovery Today*, 2015. 20: p. 595–601.
4. Lansdown, A.B., A pharmacological and toxicological profile of silver as an antimicrobial agent in medical devices. *Advances in Pharmacological Sciences*, 2010. pp. 16.
5. Goia, D.V., and E. Matijević, Preparation of monodispersed metal particles. *New Journal of Chemistry*, 1998. 11: p. 1203–1208.
6. Taleb, A., C. Petit, and M.P. Pileni, Synthesis of highly monodisperse silver nanoparticles from AOT reverse micelles: A way to 2D and 3D self-organization. *Chemistry of Materials*, 1997. 9: p. 950–959.
7. Esumi, K., et al., Preparation and characterization of bimetallic Pd-Cu colloids by thermal decomposition of their acetate compounds in organic solvents. *Chemistry of Materials*, 1990. 2: p. 564–567.
8. Henglein, A., Reduction of $\text{Ag}(\text{CN})_2$ -on silver and platinum colloidal nanoparticles. *Langmuir*, 2001. 17: p. 2329–2333.
9. Rodríguez-Sánchez, L., et al., Electrochemical synthesis of silver nanoparticles. *The Journal of Physical Chemistry B*, 2000. 104: p. 9683–9688.
10. Zhu, J., et al., Shape-controlled synthesis of silver nanoparticles by pulse sonoelectrochemical methods. *Langmuir*, 2000. 16: p. 6396–6399.
11. Pastoriza-Santos, I., and L.M. Liz-Marzán, Formation of PVP-protected metal nanoparticles in DMF. *Langmuir*, 2002. 18: p. 2888–2895.
12. Kröger, N., et al., Polycationic peptides from diatom biosilica that direct silica nanosphere formation. *Science*, 1999. 286: p. 1129–1132.
13. Ahmad, A., et al., Extracellular biosynthesis of silver nanoparticles using the fungus *Fusarium oxysporum*. *Colloids and Surfaces B: Biointerfaces*, 2003. 28: p. 313–318.
14. Shahverdi, A.R., et al., Rapid synthesis of silver nanoparticles using culture supernatants of Enterobacteria: a novel biological approach. *Process Biochemistry*, 2007. 42: p. 919–923.
15. Siddiqi, K.S., et al., Biogenic fabrication and characterization of silver nanoparticles using aqueous-ethanolic extract of lichen (*Usnea longissima*) and their antimicrobial activity. *Biomaterials Research*, 2018. 22: p. 1–9.
16. Nath, D., and P. Banerjee, Green nanotechnology—a new hope for medical biology. *Environmental Toxicology and Pharmacology*, 2013. 36: p. 997–1014.
17. Ovais, M., et al., Role of plant phytochemicals and microbial enzymes in biosynthesis of metallic nanoparticles. *Applied Microbiology and Biotechnology*, 2018. 102: p. 6799–6814.
18. Gardea-Torresdey, J.L., et al., Alfalfa sprouts: A natural source for the synthesis of silver nanoparticles. *Langmuir*, 2003. 19: p. 1357–1361.
19. Shankar, S.S., et al., Rapid synthesis of Au, Ag, and bimetallic Au core–Ag shell nanoparticles using Neem (*Azadirachta indica*) leaf broth. *Journal of Colloid and Interface Science*, 2004. 275: p. 496–502.
20. Chandran, S.P., et al., Synthesis of gold nanotriangles and silver nanoparticles using *Aloe vera* plant extract. *Biotechnology Progress*, 2006. 22: p. 577–583.
21. Vilchis-Nestor, A.R., et al., Solventless synthesis and optical properties of Au and Ag nanoparticles using *Camellia sinensis* extract. *Materials Letters*, 2008. 62: p. 3103–3105.
22. Sathishkumar, M., et al., *Cinnamon zeylanicum* bark extract and powder mediated green synthesis of nano-crystalline silver particles and its bactericidal activity. *Colloids and Surfaces B: Biointerfaces*, 2009. 73: p. 332–338.
23. Bar, H., et al., Green synthesis of silver nanoparticles using seed extract of *Jatropha curcas*. *Colloids and Surfaces A: Physicochemical and Engineering Aspects*, 2009. 348: p. 212–216.

24. Bankar, A., et al., Banana peel extract mediated novel route for the synthesis of silver nanoparticles. *Colloids and Surfaces A: Physicochemical and Engineering Aspects*, 2010. 368: p. 58–63.
25. Krishnaraj, C., et al., Synthesis of silver nanoparticles using *Acalypha indica* leaf extracts and its antibacterial activity against water borne pathogens. *Colloids and Surfaces B: Biointerfaces*, 2010. 76: p. 50–56.
26. Vidhu, V.K., S.A. Aromal, and D. Philip, Green synthesis of silver nanoparticles using *Macrotyloma uniflorum*. *Spectrochimica Acta Part A: Molecular Molecular Spectra*, 2011. 83: p. 392–397.
27. Raja, K., A. Saravanakumar, and R. Vijayakumar, Efficient synthesis of silver nanoparticles from *Prosopis juliflora* leaf extract and its antimicrobial activity using sewage. *Spectrochimica Acta Part A: Molecular Molecular Spectra*, 2012. 97: p. 490–494.
28. Geetha, A.R., et al., Optimization of green synthesis of silver nanoparticles from leaf extracts of *Pimenta dioica* (allspice). *The Scientific World Journal*, 2013: 5 p.
29. Shetty, P., et al., Synthesis, characterization and antimicrobial activity of *Alstonia scholaris* bark-extract-mediated silver nanoparticles. *Journal of Nanostructure in Chemistry*, 2014. 4: p. 161–170.
30. Pourmortazavi, S.M., et al., Procedure optimization for green synthesis of silver nanoparticles by aqueous extract of *Eucalyptus oleosa*. *Spectrochimica Acta Part A: Molecular Molecular Spectra*, 2015. 136: p. 1249–1254.
31. Ali, M., et al., Inhibition of *Phytophthora parasitica* and *P. capsici* by silver nanoparticles synthesized using aqueous extract of *Artemisia absinthium*. *Phytopathology*, 2015. 105: p. 1183–1190.
32. Ravichandran, V., et al., Green synthesis of silver nanoparticles using *Atrocarpus altilis* leaf extract and the study of their antimicrobial and antioxidant activity. *Materials Letters*, 2016. 180: p. 264–267.
33. Karthik, R., et al., Biosynthesis of silver nanoparticles by using *Camellia japonica* leaf extract for the electrocatalytic reduction of nitrobenzene and photocatalytic degradation of Eosin-Y. *Journal of Photochemistry and Photobiology B: Biology*, 2017. 170: p. 164–172.
34. Kumar, B., et al., Green synthesis of silver nanoparticles using Andean blackberry fruit extract. *Saudi Journal of Biological Sciences*, 2017. 24: p. 45–50.
35. Chahardoli, A., N. Karimi, and A. Fattahi, *Nigella arvensis* leaf extract mediated green synthesis of silver nanoparticles: Their characteristic properties and biological efficacy. *Advanced Powder Technology*, 2017. 29: p. 202–210.
36. Arya, K., et al., Green synthesis of silver nanoparticles using *Prosopis juliflora* bark extract: reaction optimization, antimicrobial and catalytic activities. *Artificial Cells, Nanomedicine, and Biotechnology*, 2018. 46: p. 985–993.
37. Satpathy, S., et al., Antioxidant and anticancer activities of green synthesized silver nanoparticles using aqueous extract of tubers of *Pueraria tuberosa*. *Artificial Cells, Nanomedicine, and Biotechnology*, 2018. 46: p. 71–85.
38. Behravan, M., et al., Facile green synthesis of silver nanoparticles using *Berberis vulgaris* leaf and root aqueous extract and its antibacterial activity. *International Journal of Biological Macromolecules*, 2019. 124: p. 148–154.
39. Maghsoudy, N., et al., Biosynthesis of Ag and Fe nanoparticles using *Erodium cicutarium*; study, optimization, and modeling of the antibacterial properties using response surface methodology. *Journal of Nanostructure in Chemistry*, 2019. 9: p. 203–216.
40. Ghojavand, S., M. Madani, and J. Karimi, Green synthesis, characterization and antifungal activity of silver nanoparticles using stems and flowers of Felty germander. *Journal of Inorganic and Organometallic Polymers and Materials*, 2020. 30: p. 2987–2997.

41. Venkatadri, B., et al., Green synthesis of silver nanoparticles using aqueous rhizome extract of *Zingiber officinale* and *Curcuma longa*: In-vitro anti-cancer potential on human colon carcinoma HT-29 cells. *Saudi Journal of Biological Sciences*, 2020. 27: p. 2980–2986.
42. Fatimah, I., et al., Ultrasound-assisted biosynthesis of silver and gold nanoparticles using *Clitoria ternatea* flower. *South African Journal of Chemical Engineering*, 2020. 34: p. 97–106.
43. Bharadwaj, K.K., Green synthesis of silver nanoparticles using *Diospyros malabarica* fruit extract and assessments of their antimicrobial, anticancer and catalytic reduction of 4-nitrophenol (4-np). *Nanomaterials*, 2021. 11: p. 1999.
44. Al-Otibi, F., et al., Biosynthesis of silver nanoparticles using *Malva parviflora* and their antifungal activity. *Saudi Journal of Biological Sciences*, 2021. 28: p. 2229–2235.
45. Le, N.T.T., et al., The physicochemical and antifungal properties of eco-friendly silver nanoparticles synthesized by *Psidium guajava* leaf extract in the comparison with *Tamarindus indica*. *Journal of Cluster Science*, 2021. 32: p. 601–611.
46. Kolaylı, S., et al., Chemical and antioxidant properties of *Laurocerasus officinalis* Roem. (cherry laurel) fruit grown in the Black Sea Region. *Journal of Agricultural and Food Chemistry*, 2003. 51: p. 7489–94.
47. Yesilada, E., et al., Traditional medicine in Türkiye IX. Folk Medicine in North-West Anatolia. *Journal of Ethnopharmacology*, 1999. 64: p. 195–210.
48. Şahan, Y., Effect of *Prunus laurocerasus* L. (cherry laurel) leaf extracts on growth of bread spoilage fungi. *Bulgarian Journal of Agricultural Science*, 2011. 17: p. 83–92.
49. Karabegovic, I.T., et al., The effect of different extraction techniques on the composition and antioxidant activity of cherry laurel (*Prunus laurocerasus*) leaf and fruit extracts. *Industrial Crops and Products*, 2014. 54: p. 142–148.
50. Cochran, W.G., and G.M. Cox, *Experimental designs*, 2nd ed. New York: Wiley, 1992. pp. 335–375.
51. Türkkän, M., Antifungal effect of various salts against *Fusarium oxysporum* f. sp. *cepae*, the causal agent of *Fusarium* basal rot of onion. *Journal of Agricultural Sciences*, 2013. 19: p. 178–187.
52. Thompson, D.P., Fungitoxic activity of essential oil components on food storage fungi. *Mycologia*, 1989. 81: p. 151–153.
53. Tripathi, P., et al., Evaluation of some essential oils as botanical fungi toxicants in management of post-harvest rotting of citrus fruits. *World Journal of Microbiology and Biotechnology*, 2004. 20: p. 317–321.
54. Vanaja, M., et al., Phytosynthesis of silver nanoparticles by *Cissus quadrangularis*: influence of physicochemical factors. *Journal of Nanostructure in Chemistry*, 2013. 3: p. 1–8.
55. Veerasamy, R., et al., Biosynthesis of silver nanoparticles using mangosteen leaf extract and evaluation of their antimicrobial activities. *Journal of Saudi Chemical Society*, 2011. 15: p. 113–120.
56. Reddy, L.V.A., et al., Optimization of alkaline protease production by batch culture of *Bacillus* sp. RKY3 through Plackett–Burman and response surface methodological approaches. *Bioresource Technology*, 2008. 99: p. 2242–2249.
57. Mondal, P., and M.K. Purkait, Green synthesized iron nanoparticle-embedded pH-responsive PVDF-co-HFP membranes: optimization study for NPs preparation and nitrobenzene reduction. *Separation Science and Technology*, 2017. 52: p. 2338–2355.
58. Sun, Q., et al., Green synthesis of silver nanoparticles using tea leaf extract and evaluation of their stability and antibacterial activity. *Colloids and Surfaces A: Physicochemical and Engineering Aspects*, 2014. 444: p. 226–231.
59. Sanghi, R., and P. Verma, Biomimetic synthesis and characterisation of protein capped silver nanoparticles. *Bioresource Technology*, 2009. 100: p. 501–504.

60. Nikaeen, G., et al., Central composite design for optimizing the biosynthesis of silver nanoparticles using *Plantago major* extract and investigating antibacterial, antifungal and antioxidant activity. *Scientific Reports*, 2020. 10: p. 1–16.
61. Mulvaney, P., Surface plasmon spectroscopy of nanosized metal particles. *Langmuir*, 1996. 12: p. 788–800.
62. Njagi, E.C., et al., Biosynthesis of iron and silver nanoparticles at room temperature using aqueous sorghum bran extracts. *Langmuir*, 2011. 27: p. 264–271.
63. Gurunathan, S., et al., Multidimensional effects of biologically synthesized silver nanoparticles in *Helicobacter pylori*, *Helicobacter felis*, and human lung (L132) and lung carcinoma A549 cells. *Nanoscale Research Letters*, 2015. 10: p. 35.
64. Jeeva, K., et al., *Caesalpinia coriaria* leaf extracts mediated biosynthesis of metallic silver nanoparticles and their antibacterial activity against clinically isolated pathogens. *Industrial Crops and Products*, 2014. 52: p. 714–720.
65. Reddy, N.J., et al., Evaluation of antioxidant, antibacterial and cytotoxic effects of green synthesized silver nanoparticles by *Piper longum* fruit. *Materials Science and Engineering: C*, 2014. 34: p. 115–122.
66. Magudapathy, P., et al., Electrical transport studies of Ag nanoclusters embedded in glass matrix. *Physica B: Condensed Matter*, 2001. 299: p. 142–146.
67. Krishnaraj, C., et al., Optimization for rapid synthesis of silver nanoparticles and its effect on phytopathogenic fungi. *Spectrochimica Acta Part A: Molecular and Biomolecular Spectroscopy*, 2012. 93: 95–99.
68. Buzea, C., I.I. Pacheco, and K. Robbie, Nanomaterials and nanoparticles: sources and toxicity. *Biointerphases*, 2007. 2: p. 17–64.